AGN in the XMM-Newton first-light image as probes for the interstellar medium in the LMC*

F. Haberl[1], K. Dennerl[1], M.D. Filipović[1,2,3], B. Aschenbach[1], W. Pietsch[1], and J. Trümper[1]

[1] Max-Planck-Institut für extraterrestrische Physik, Giessenbachstraße, 85748 Garching, Germany
[2] University of Western Sydney Nepean, P.O. Box 10, Kingswood, NSW 2747, Australia
[3] Australia Telescope National Facility, CSIRO, P.O. Box 76, Epping, NSW 2121, Australia

Abstract. The XMM-Newton first-light image revealed X-ray point sources which show heavily absorbed power-law spectra. The spectral indices and the probable identification of a radio counterpart for the brightest source suggest AGN shining through the interstellar gas of the Large Magellanic Cloud (LMC). The column densities derived from the X-ray spectra in combination with H I measurements will allow to draw conclusions on H I to H_2 ratios in the LMC and compare these with values found for the galactic plane.

Key words. Galaxies: LMC – Quasars: general – X-rays: ISM

1. Introduction

The study of active galactic nuclei and quasi stellar objects (both named AGN hereafter) behind nearby galaxies allows to probe the interstellar matter in the foreground galaxy. Absorption lines in optical spectra provide information about the absorbing material along the line of sight through the galaxy. However, very few AGN are known behind nearby galaxies as surveys for these objects avoided the crowded fields. Dedicated searches for AGN behind nearby galaxies were performed by Tinney et al. (1997) and Crampton et al. (1997). Conducting optical identification programs of ROSAT X-ray sources, they found 15 background objects in the direction of the Small Magellanic Cloud and 11 towards the LMC involving also clusters of galaxies and individual distant galaxies. For all these background objects red-shifts were determined covering the range of 0.02 − 2.3. From more general optical identification programs of X-ray sources in the Magellanic Clouds by Cowley et al. (1984, 1997) and Schmidtke et al. (1999) further AGN were found and X-ray classification work by Haberl & Pietsch (1999) and Haberl et al. (2000) suggests candidates for background objects based on their X-ray (and radio) properties. However, as consequence of the strong attenuation of X-rays in the ROSAT 0.1 − 2.4 keV band by interstellar matter which hampers the X-ray detection of AGN in the dense cores (where column densi-

ties of the order of 10^{22} cm^{-2} are expected which suppress the flux at 1 keV by a factor ∼10 and at 0.4 keV by more than 10^4), the background objects were mainly found in the outer regions of the Magellanic Clouds.

The high sensitivity and good spectral resolution of the EPIC instruments on board of XMM-Newton (Jansen et al. 2001) over a wide energy band from 0.1 keV up to 15 keV provides a unique tool to detect hard (intrinsically and/or highly absorbed) X-ray sources and allows for the first time to separate very accurately the intrinsic X-ray source spectrum (determined from higher energies) and the photo-electric absorption which attenuates the spectrum at lower energies. The EPIC instruments are therefore ideally suited to investigate the absorbing matter in the dense cores of nearby galaxies by observing AGN behind the galaxies. While radio observations in the 21 cm line infer the column density of H I only (e.g. Arabadijs & Bregman 1999), X-ray absorption measurements provide a linear measure of the total mass along the line of sight.

In this letter we report on a sample of highly absorbed point sources detected in the XMM-Newton first-light image obtained by the EPIC-PN camera (Strüder et al. 2001) south-west of the 30 Doradus region in the LMC. Their X-ray spectra strongly suggest AGN as origin of the X-rays.

2. Data analysis and results

2.1. XMM-Newton first light

XMM-Newton received first light from a region of the LMC centered between the supernova remnants (SNRs)

Table 1. XMM-Newton/EPIC-PN first-light observations of the LMC

Date 2000 January	Filter	Pointing Centre (J2000) RA[h m s], Dec[° ′ ″]
19 16:19-17:22	medium	05 36 57, −69 13 47
19/20 17:30-04:27	medium	05 36 57, −69 13 47
21 15:37-19:37	medium	05 37 04, −69 13 00
21/22 20:32-07:00	thin1	05 37 04, −69 13 00
22 09:07-12:01	thin1	05 37 04, −69 13 00

Table 2. Hard X-ray point sources

	RA (J2000) [h m s]	Dec (J2000) [° ′ ″]	CR[1]	HR	Flux[2]
1	05 36 50.7	−69 16 40			
2	05 36 56.4	−69 11 49	3.8	0.45±0.23	1.6
3	05 36 58.1	−69 13 43	25.1	1.16±0.06	19
4	05 37 09.2	−69 13 00	3.2	1.60±0.22	3.4
5	05 37 16.7	−69 13 33	3.9	3.00±0.24	4.4
6	05 37 22.3	−69 15 31	5.2	0.55±0.15	3.1
7	05 37 27.9	−69 20 47	3.7	0.57±0.68	1.9
8	05 37 30.5	−69 19 04	3.6	0.35±0.19	2.1
9	05 38 00.2	−69 16 28	3.7	0.66±0.25	1.4

[1] Count rate in 10^{-3} s^{-1} in the 0.3 – 10 keV band
[2] 0.3 – 10 keV flux in 10^{-14} erg cm^{-2} s^{-1}

N 157B and SN 1987A. The field was observed five times with the EPIC-PN instrument in January 2000 using different optical light blocking filters and slightly different pointing positions (Tab. 1). The particular field in the LMC was chosen because of its richness of X-ray emission seen already by the Einstein (Wang et al. 1991) and ROSAT (Trümper et al. 1991) satellites. Besides diffuse emission from hot interstellar gas and emission from extended sources like SNRs, the first-light image revealed point sources which appear green and blue in the energy-colour coded image (Fig. 1). The colours indicate sources with hard X-ray spectrum as expected from X-ray binaries residing in the LMC or background AGN shining through the interstellar gas and dust of the LMC.

First attempts of source detection using sliding window techniques revealed at least a dozen of point sources. The brightest nine are summarized in Table 2 and marked in Fig. 1. The X-ray position was derived after alignment (translation only) of the image to match the coordinates of SN 1987A. Systematic errors of up to 15″ can be introduced by an uncertain rotation of the image of the order of 2° which is required to match the individual images. The coordinates in Table 2 should therefore be regarded as preliminary. A hardness ratio to characterize the X-ray spectrum was obtained by dividing the counts in the 2.0 − 10.0 keV and 0.5 − 2.0 keV bands. As expected the blue sources in the colour image show highest hardness ratios above 1.0 while the green sources have values around 0.5.

To derive X-ray spectra we merged the first two and the last two observations which had identical in-
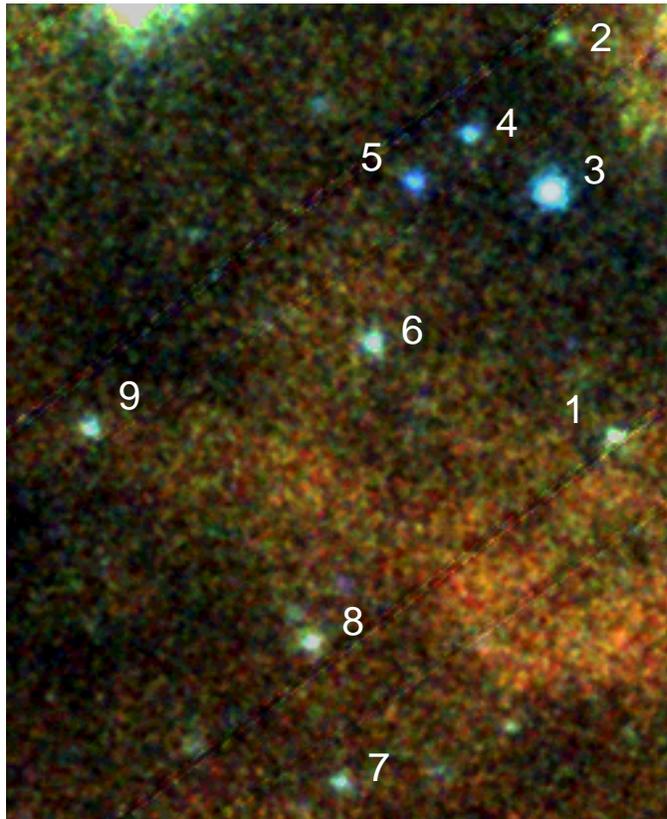
Fig. 1. Section (7.7′ x 9.5′) of the EPIC-PN first-light image with the investigated point sources marked. The photon energy is coded in colour from 0.3 keV (red) to 5.0 keV (blue). The bright source in the upper-left is N 157B. North is up and east to the left. For the full image and further details on the production see Dennerl et al. (2001)

strumental configurations. For each of the three resulting data sets a spectrum was derived from source and nearby background regions. Only for the brightest source J0536.9−6913 (source 3), close to the center of the field of view, spectra with sufficient statistics for a spectral fit were obtained. The three spectra were simultaneously fit with a power-law model attenuated by photo-electric absorption. A column density with equivalent N_H of $6\cdot10^{20}$ cm^{-2} (Dickey et al. 1990) with solar abundance was assumed (fixed in the fit) for the galactic foreground absorption. For the LMC absorption (free in the fit) a metallicity of 0.5 solar (Russell & Dopita 1992) was used. Spectra and best-fit model (histogram) are shown in Fig. 2. Since no photon arrival times were available in the first processing version of the data, no exposure correction was applied to the spectra. The strong turn-over of the spectrum is caused by high photo-electric absorption.

To increase photon statistics we merged spectra from sources with similar hardness ratios. Sources 4 and 5 are located close to J0536.9−6913 (source 3) and show the highest hardness ratios. We also merged the spectra of sources 6, 8 and 9 with hardness ratios between 0.35 and 0.66. Again, highly absorbed power-law models were found to fit the spectra satisfactory (see Table 3 where N_H and
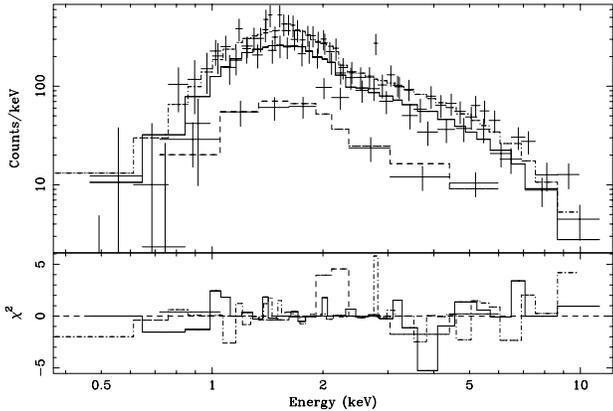
Fig. 2. EPIC-PN spectra of J0536.9−6913 (source 3) obtained from three different data sets together with the best fit model as histogram (solid: merged observations 1 and 2, medium filter; dash: observation 3, medium filter; dash-dot: observations 4 and 5, thin filter). The different normalizations reflect the different exposure times
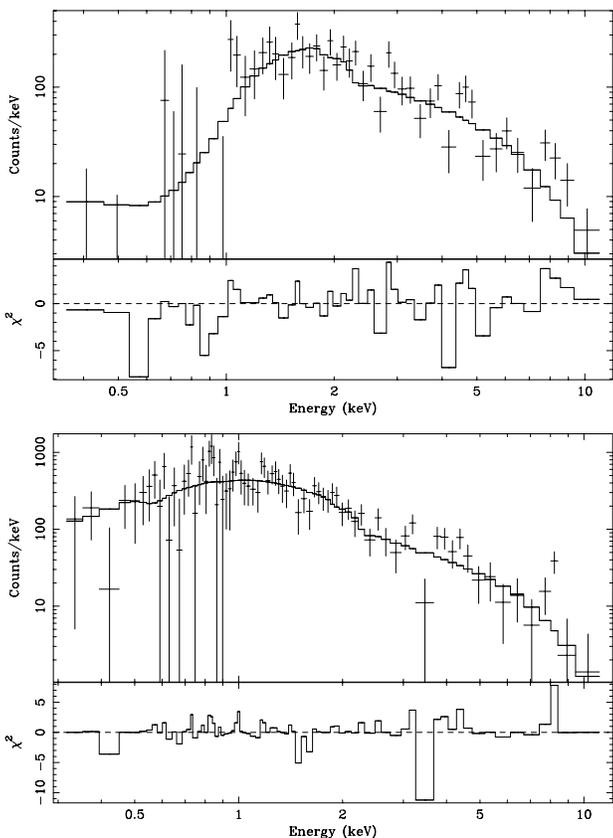
Fig. 3. EPIC-PN spectra of point sources detected in the first light image: combined J0537.1−6913 and J0537.2−6913 (top) and combined J0537.3−6915, J0538.0−6916 and J0537.5−6919 (bottom)

photon index γ are listed). For better comparison and presentation the three spectra from the individual data sets were merged into a single spectrum. These are shown for the combined sources in Fig. 3. The model is plotted using an average response matrix. The combined spectrum of

Table 3. Spectral parameters for a power-law model

Source	N_H [10^{22} cm^{-2}]	γ	χ^2/dof
3	1.69±0.25	1.97±0.16	80.7/85
4/5	2.26±0.75	1.75±0.32	69.8/49
6/8/9	0.35±0.13	1.78±0.23	93.8/77

sources 6, 8 and 9 clearly suffers less absorption compared to the spectrum of J0536.9−6913 (source 3) as indicated by the hardness ratios and quantified by the N_H derived from the spectral fits.

To estimate the exposure times of the observations we produced EPIC-PN spectra of the SNR N157B and normalized their flux in the 0.3 − 2.4 keV band to a ROSAT PSPC spectrum of this source. Unfortunately during the first two XMM observations N157B was located on a CCD border and flux was lost. Therefore, we only used the third part of the observations (the two thin filter observations) for this purpose where we found a net exposure of 31.0 ks. Source count rates and fluxes listed in Table 2 are derived from the merged thin filter observations using this exposure. The fluxes (0.3 − 10 keV) were derived from the spectral fits using the parameters given in Table 3. For those sources without spectral fit the parameters from the combined fit including J0537.3−6915 were used, i.e. low absorption compatible with the hardness ratios.

2.2. The radio source ATCA J0536.9−6913 = J0536.9−6913

The region around J0536.9−6913 was observed as part of ATCA mosaic observations of the LMC with a baseline of 1500 m at frequencies of 1420 and 2370 MHz with angular resolutions of ∼45″ and ∼30″. Similar ATCA observations in 'snap-shot mode' at 4800 MHz were undertaken for specific regions including J0536.9−6913 (Filipović & Staveley-Smith 1998). The baseline of these observations was 375 m with resolutions of ∼30″ and ∼15″, respectively. An additional observation of this region was made at 843 MHz with the Molonglo Synthesis Telescope (MOST) (Mills 1981) as part of LMC survey and SN 1987A monitoring projects at this frequency.

Radio-continuum emission from a point-like source is detected at RA = 05^h 36^m 56^{s}62 and Dec = −69° 13′ 27″7 (J2000), compatible with the X-ray position given the uncertainty in position angle of the X-ray image. The integrated flux density of this source, designated ATCA J0536.9−6913, at 843, 1420, 2370 and 4800 MHz was determined to 336±30, 211±20, 116±11 and 102±10 mJy, respectively.

We derive a spectral index α = 0.73±0.16 (defined by $S_\nu \sim \nu^{-\alpha}$) from the flux densities, S_ν, at the frequencies, ν, of 843, 1420, 2370 and 4800 MHz (Fig. 4). This spectral index is typical for radio background sources which are mainly AGN or radio quasars (Filipović et al. 1998).
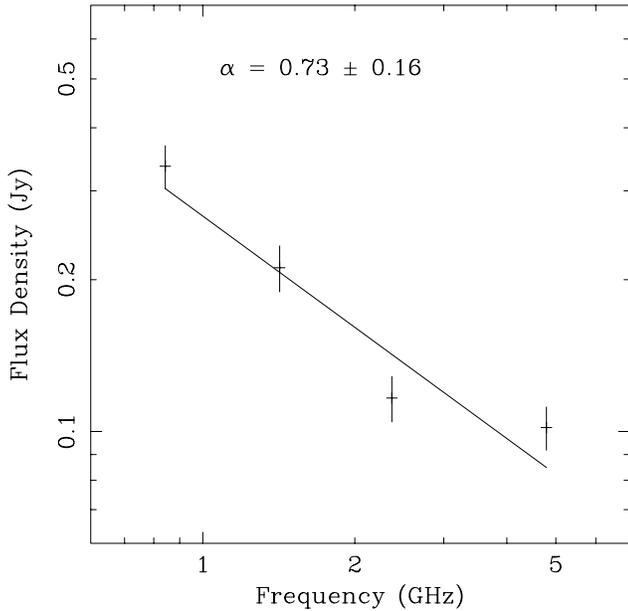
Fig. 4. Radio spectrum of ATCA J0536.9−6913 = J0536.9−6913

3. Discussion

We investigated nine point sources with hard X-ray spectra detected in the XMM-Newton first-light images. Their X-ray spectra can be represented by highly absorbed power-laws and the derived photon indices between 1.7 and 2.0 are typical for steep AGN spectra (e.g. Vaughan et al. 1999). In contrast accreting high mass X-ray binaries show harder X-ray spectra with typical indices between 0 and 1 (e.g. Yokogawa et al. 2000) not compatible with the indices found for our point sources. The radio spectral index of 0.73 found for J0536.9−6913 also supports the AGN interpretation.

AGN spectra sometimes show intrinsic absorption which can easily reach the amount seen in the spectra reported here. So the question remains which fraction of the column density can be attributed to the LMC. The fact that the three close point sources near the center of the field of view all show similar high absorption of the order of 10^{22} cm^{-2} suggests that most of the N_H is intrinsic to the LMC. The derived column density of $0.35 \cdot 10^{22}$ cm^{-2} of sources only ∼2′ away from the central sources shows that the absorption can change by a factor of more than 5 over distances of ∼30 pc in the LMC. It is remarkable in this respect that the north-west part of the first-light image lacks of point sources. This suggests that even higher column densities exceeding 10^{22} cm^{-2} are required to suppress the detection of AGN in that region.

X-ray absorption measurements are directly related to the total hydrogen column density, comprising H I, H$_2$ and H II column densities. Because the absorbing elements at X-ray energies are He and metals their relative abundance must be taken into account to derive X-ray hydrogen column densities. This was done in our spectral fits assuming abundances of 0.5 relative to solar (Russell & Dopita

1992). Kim et al. (2000) have produced a H I column density map of the LMC with a resolution of 1′ which shows variations from 0 to $5 \cdot 10^{21}$ cm^{-2} with maximum values around the 30 Doradus region. The higher absorption seen in the XMM sources suggests either large amounts of H II and/or H$_2$ gas or higher metal abundances along their lines of sight through the LMC. Higher abundances of O, Ne, Mg and Si in the interstellar medium are suggested by the spectrum of the diffuse emission near the 30 Dor region (Dennerl et al. 2001).

References

Arabadjis, J.S., & Bregman, J.N. 1999, ApJ, 510, 806
Cowley, A.P., Crampton, D., Hutchings, J.B., et al. 1984, ApJ, 286, 196
Cowley, A.P., Schmidtke, P.C., McGrath, T.K., et al. 1997, PASP, 109, 21
Crampton, D., Gussie, G., Cowley, A.P., Schmidtke, P.C. 1997, AJ, 114, 2353
Dennerl, K., Haberl, F., Aschenbach, B., et al. 2001, A&A, 365 (this issue)
Dickey, J.M., & Lockman, F.J. 1990, Ann. Rev. Astron. Astrophys., 28, 215
Filipović, M.D., Haynes, R.F., White, G.L., Jones, P.A. 1998, A&AS, 130, 421
Filipović, M.D., & Staveley-Smith, L. 1998, in The Magellanic Clouds and Other Dwarf Galaxies, ed. T. Richtler, & J.M. Braun, Shaker Verlag, Aachen, 137
Haberl, F., Filipović, M.D., Pietsch, W., Kahabka, P. 2000, A&AS, 142, 41
Haberl, F., & Pietsch, W. 1999, A&AS, 139, 277
Jansen, F., Lumb, D., Altieri, B., et al. 2001, A&A, 365 (this issue)
Kim, S., Staveley-Smith, L., Sault, R.J. 2000, in ASP Conf. Ser. (in press), Gas and Galaxy Evolution, ed. J.E. Hibbard, M.P. Rupen, J.H. van Gorkom, astro-ph/0009299
Mills, B.Y. 1981, PASA, 4, 156
Russell, S.C., & Dopita, M.A. 1992, ApJ, 384, 508
Schmidtke, P.C., Cowley, A.P., Crane, J.D., et al. 1999, AJ, 117, 927
Strüder, L., Briel, U., Dennerl, K., etal. 2001, A&A, 365 (this issue)
Tinney, C.G., Da Costa, G.S., Zinnecker, H. 1997, MNRAS, 285, 111
Trümper, J., Hasinger, G., Aschenbach, B., et al. 1991, Nature, 349, 579
Vaughan, S., Reeves, J., Warwick, R., Edelson, R. 1999, MNRAS, 309, 113
Wang, Q., Hamilton, T., Helfand, D.J., Wu, X. 1991, ApJ, 374, 475
Yokogawa, J., Imanishi, K., Tsujimoto, M., et al. 2000, ApJS, in press, astro-ph/0002167